Dalton Transactions

Accepted Manuscript

ROYAL SOCIETY OF CHEMISTRY

www.rsc.org/dalton

Dalton Transactions

PAPER

C_2H_2 Adsorption in Three Isostructural Metal-Organic Frameworks: Boosting C_2H_2 Uptake by Rational Arrangement of Nitrogen Sites

Received 00th January 20xx,
Accepted 00th January 20xx

DOI: 10.1039/x0xx00000x

www.rsc.org/

Chengling Song, Jingjing Jiao, Qiyi Lin, Huimin Liu, and Yabing He*

Replacing the benzene spacer in the organic linker 5,5'-(benzene-1,4-diyl)diisophthalate with the nitrogen containing heterocyclic rings, namely, pyrazine, pyridazine, and pyrimidine results in three organic linkers, which were reacted with copper ions under solvothermal conditions to form three isostructual metal-organic frameworks (ZJNU-46, ZJNU-47 and ZJNU-48) exhibiting exceptionally high sorption capacities with regard to acetylene due to the simultaneous immobilization of open metal sites and Lewis basic nitrogen sites in the frameworks. At 1 atm and 295 K, the gravimetric C_2H_2 adsorption uptakes reach 187, 213 and 193 cm^3(STP) g^{-1} for these three compounds. The gravimetric C_2H_2 adsorption amount of **ZJNU-47a** is the second highest reported for MOF materials. Notably, despite their same porosities, and densities of open metal sites and uncoordinated nitrogen sites, distinctly different C_2H_2 adsorption capacities were observed for these three compounds, which we think is mainly associated with the difference in the relative position of nitrogen atoms leading to different binding affinity of the frameworks towards C_2H_2 guest molecules, and thus different C_2H_2 adsorption. This work demonstrates that the rational arrangement of open nitrogen sites will favorably improve C_2H_2 uptakes and thus provides useful information for future design of porous MOFs with high acetylene storage capacities.

1. Introduction

Acetylene is an industrially important gas which is widely used as a fuel in welding technologies and also as a very important feedstock for the synthesis of various fine chemicals and electronic materials. Despite its importance and widespread use, there remain significant issues regarding acetylene storage and transportation due to its intrinsic highly explosive characteristics. It is well known that pure acetylene stored at pressure above 0.2 MPa risks exploding at room temperature, even in the absence of oxygen. The current method of storing acetylene involves dissolution of the gas in acetone placed in a vessel along with an absorbent. However, the volatile solvent contamination restricts its use in fine chemical products and electronic materials. Therefore, there is a need for the discovery of better materials that offer enhanced capacities for safe storage of acetylene. In this regard, metal-organic frameworks (MOFs), which consist of metal ions or metal-containing clusters (typically termed as secondary building units (SBUs)) connected by multi-dentate organic linkers to form multi-dimensional network, are likely the promising candidates to solve these issues because MOFs provide opportunity for precise pore size tuning and direct pore surface engineering, which is quite difficult for traditional porous materials such as zeolites and activated carbons. In principle, the pore sizes of MOFs can be systematically tuned by selecting the diverse metal-containing SBUs and the rich organic linkers and/or by making use of framework interpenetration in the assembly process,[1] while the pore surfaces of MOFs could be designed by the controlled immobilization of a variety of organic functional sites such as NH_2, OH, COOH, etc., to adsorb specific molecules.[2] In fact, many studies on porous MOFs have demonstrated their enormous potential for the storage of various gases such as hydrogen,[3] methane,[4] CO_2,[2b, 5] and light hydrocarbons.[6]

Since Kitagawa *et al.* firstly studied acetylene adsorption in a microporous MOF material $[Cu_2(pzdc)_2(pyz)]$,[7] design and synthesis of porous MOFs for acetylene storage have drawn increasing attention from chemists.[8] For example, Xiang *et al.* systematically investigated a series of MOFs with different structures and porosities for acetylene adsorption, and evidenced the open metal sites (OMSs) are the preferential adsorption sites in MOFs.[9] Recognizing the importance of the OMSs in acetylene storage, they subsequently evaluated the acetylene adsorption properties of MOF-74 series bearing the highest concentrations of OMSs, and identified CoMOF-74 as the highest volumetric acetylene storage material.[10] Besides the OMSs, the suitable pore space is also found to play a crucial role in acetylene adsorption, which has been well demonstrated in a MOF material FJI-H8 recently reported by Yuan *et al.*, which displayed a record-high gravimetric acetylene uptake and the second-highest volumetric uptake at 295 K and 1 atm.[11] Due to the acidic nature of acetylene,

College of Chemistry and Life Sciences, Zhejiang Normal University, Jinhua 321004, China. E-mail: heyabing@zjnu.cn

Electronic Supplementary Information (ESI) available: PXRD (Fig. S1), TGA (Fig. S2), BET and Langmuir plots (Fig. S3), fitting C_2H_2 adsorption data with Langmuir-Freundlich model (Fig. S4), Vant' Hoff isochores for C_2H_2 adsorption (Fig. S5), FTIR (Fig. S6), NMR spectra (Fig. S7), crystal data and structure refinement parameters (Table S1). CCDC No. 1056732, 1441682. See DOI: 10.1039/x0xx00000x

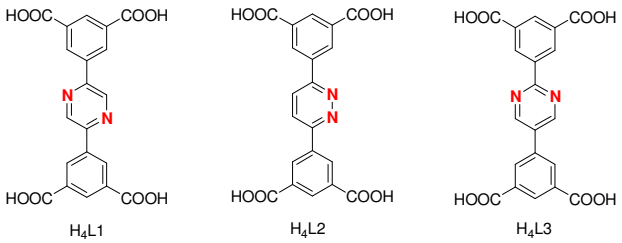

Scheme 1 The organic linkers used to construct **ZJNU-46**, **ZJNU-47** and **ZJNU- 48**.

functionalization of the organic linkers constituting MOFs with Lewis basic functional groups also appears to be a logical solution to boost the C_2H_2 uptake. By employing this approach, Rao *et al.* synthesized a MOF ZJU-5 incorporating Lewis basic pyridyl sites exhibiting high acetylene uptake of 290 cm^3 (STP) g^{-1} at 273 K and 1 bar.[12] These studies have revealed that creation of the OMSs, construction of suitable pore space and ligand functionalization represents three effective strategies to improve the overall acetylene adsorption capacities in MOFs. Although significant progress has been made and some MOFs have been identified as efficient acetylene storage materials, systematic studies on their structure-performance relationship in MOFs of a given structure have been less performed experimentally. The study in this aspect will certainly facilitate the discovery of new porous MOFs with high acetylene storage capacities.

Recently, we used a diisophthalate organic ligand, 5,5'-(pyridazine-3,6-diyl)-diisophthalate (H_4L2, Scheme 1), to synthesize a MOF **ZJNU-47** featuring high density of OMSs (1.56 nm^{-3}) and Lewis basic nitrogen donor sites (1.56 nm^{-3}), which exhibits the highest acetylene uptake of 300 cm^3 (STP) g^{-1} at 273 K and 1 atm.[13] To investigate and understand the effect the relative position of nitrogen atoms have on acetylene adsorption, we have designed and synthesized two more diisophthalate organic linkers H_4L1 and H_4L3 shown in Scheme 1. Different with the organic linker H_4L2 used to construct a MOF **ZJNU-47**, the relative position of nitrogen atoms on the spacer between the terminal isophthalate moieties in the organic ligands H_4L1 and H_4L3 was changed from "*ortho-*" to "*para-*" and "*meta-*", respectively. By using the organic linkers H_4L1 and H_4L3, we successfully targeted the corresponding isostructural NbO-type MOFs we termed **ZJNU-46** and **ZJNU-48**, respectively. It should be mentioned that the latter compound has been reported by Li and co-workers, but their work mainly focused on methane storage.[14] In the present work, we pay much attention on its acetylene adsorption. Herein, we wish to report on their synthesis, structural characterization as well as acetylene adsorption properties. The systematic studies of acetylene adsorption in the three isostructural MOFs revealed that the rational design of Lewis basic nitrogen sites will favourably improve the C_2H_2 uptakes.

2. Experimental

2.1 Materials and measurements

All reagents and solvents were purchased from commercial sources and used as received without further purification unless otherwise specified. Dimethyl (5-pinacolboryl)isophthalate was synthesized according to the reported method.[4a] ^1H and ^{13}C NMR spectra were recorded at a Bruke Avance 600 or 400 spectrometer at room temperature. Infrared spectra (FTIR) were recorded in the 4000-400 cm^{-1} region on a Nicolet 5DX FTIR spectrometer using KBr pellets. Elemental analyses (C, H and N) were performed using a Perkin–Elmer 240 CHN analyser. Thermogravimetric analysis (TGA) was performed under a flowing nitrogen atmosphere with a Netzsch STA 449C thermal analyser at a heating rate of 5 K min^{-1} in the temperature range from room temperature to 1073 K. The powder X-ray diffraction measurement was recorded on a Philips PW3040/60 automated powder diffractometer using Cu-K_α radiation (λ = 1.542 Å) at room temperature. Low-pressure gas adsorption isotherms were investigated with a Micrometrics ASAP 2020 HD88 surface area and porosity analyser using the extra-high pure gases. The gases used had the following specifications (volume percentage): N_2 99.9999%, and C_2H_2 99.9%. The sorption measurement was maintained at 77 K with liquid nitrogen and at other specified temperatures by a circulating bath (Julabo F12).

2.2 synthesis and characterization of the organic linkers

5,5'-(pyrazine-2,5-diyl) diisophthalate (H_4L1): To a mixture of 2,5-dibromopyrazine (1.00 g, 4.2 mmol), dimethyl (5-pinacolboryl)isophthalate (2.96 g, 9.2 mmol), $Pd(PPh_3)_4$ (0.24 g, 0.2 mmol) and Cs_2CO_3 (4.11 g, 12.6 mmol) were added degassed dioxane (100 mL). The resulting suspension was refluxed for 72 h under a nitrogen atmosphere. After that, the precipitate was collected by filtration, washed with 1,4-dioxane and then recrystallized with toluene to obtain pure tetramethyl ester intermediate as an off-while solid in 45% yield (0.88 g, 1.9 mmol). To tetramethyl ester intermediate (0.88 g, 1.9 mmol) in THF (30 mL) and methanol (30 mL) was added 6 M NaOH aqueous solution (30 mL, 180 mmol). The mixture was stirred under reflux overnight. After the solution was cooled to room temperature, the solvent was rato-evaporated, and the residue was re-dissolved in water, and filtered. The filtrate was acidified with concentrated HCl under ice-water bath. The precipitation formed was collected by filtration and dried under vacuum at 343 K, affording 5,5'-(pyrazine-2,5-diyl) diisophthalate as an off-white solid in a quantitative yield (0.75 g, 1.8 mmol). ^1H NMR (DMSO-d_6, 400.1 MHz) δ (ppm): 13.523 (s, br, 4H), 9.529 (s, 2H), 8.958 (d, J = 1.2 Hz, 4H), 8.586 (d, J = 1.2 Hz, 2H); ^{13}C NMR (DMSO-d_6, 150.9 MHz) δ (ppm): 166.840, 149.212, 142.120, 137.021, 132.923, 131.620, 131.502; selected FTIR (KBr, cm^{-1}): 1716, 1605, 1498, 1456, 1435, 1327, 1279, 1248, 1161, 1039, 910, 758, 712, 677.

5,5'-(pyrimidine-2,5-diyl) diisophthalate (H_4L3): To a mixture of 5-bromo-2-iodopyrimidine (1.19 g, 4.2 mmol), dimethyl (5-pinacolboryl)isophthalate (2.96 g, 9.2 mmol), $Pd(PPh_3)_4$ (0.24 g, 0.2 mmol) and Cs_2CO_3 (4.11 g, 12.6 mmol) were added degassed dioxane (100 mL). The resulting suspension was stirred under reflux under a nitrogen atmosphere for 72 h.

After that, the precipitate was collected by filtration, washed with 1,4-dioxane and then recrystallized with toluene to obtain pure tetramethyl ester intermediate as a white solid in 58% yield (1.13 g, 2.4 mmol). ^{1}H NMR ($CDCl_3$, 400.1 MHz) δ (ppm): 9.386 (d, *J* = 1.6 Hz, 2H), 9.158 (s, 2H), 8.863 (t, *J* = 1.6 Hz, 1H), 8.804 (t, *J* = 1.6 Hz, 1H), 8.538 (d, *J* = 1.6 Hz, 2H), 4.041 (s, 6H), 4.038 (s, 6H). To the tetramethyl ester intermediate (0.23 g, 0.5 mmol) in THF (30 mL) and methanol (30 mL) was added 6 M NaOH aqueous solution (30 mL, 180 mmol). The mixture was stirred under reflux overnight. After the solution was cooled to room temperature, the solvent was rato-evaporated, and the residue was re-dissolved in water, and filtered. The filtrate was acidified with concentrated HCl under ice-water bath. The precipitation formed was collected by filtration and dried under vacuum at 343 K, affording 5,5'-(pyrimidine-2,5-diyl) diisophthalate as an off-white solid in a quantitative yield (0.20 g, 0.5 mmol). ^{1}H NMR (DMSO-d_6, 600.1 MHz) δ (ppm): 9.394 (s, 2H), 9.219 (d, *J* = 1.2 Hz, 2H), 8.620 (t, *J* = 1.2 Hz, 1H), 8.566 (s, 3H); ^{13}C NMR (DMSO-d_6, 150.9 Hz) δ (ppm): 166.832, 166.814, 161.507, 156.343, 137.999, 135.216, 133.084, 132.622, 132.567, 132.409, 131.948, 130.936, 130.505; selected FTIR (KBr, cm^{-1}): 1713, 1605, 1551, 1454, 1406, 1385, 1271, 1255, 1234, 1157, 1105, 912, 756, 677, 661.

2.3 Synthesis and characterization of the MOFs

ZJNU-46: A mixture of H_4L1 (5.0 mg, 12.2 μmol), and $Cu(NO_3)_2{\cdot}3H_2O$ (15.0 mg, 62.1 μmol) was dissolved in a mixed solvent of *N*,*N*-dimethyl formamide (DMF, 1.5 mL), ethanol (EtOH, 0.5 mL), and H_2O (0.08 mL) in a 20 mL glass vial. After the addition of 6 M HCl (50 μL), the vial was sealed and heated to 353 K for 24 h and then cooled to room temperature. The block-shaped crystals formed were collected by filtration in 62% yield. Based on the single-crystal X-ray structural determination, TGA and elemental analysis, **ZJNU-46** can be best formulated as $[Cu_2L1(H_2O)_2]{\cdot}3DMF{\cdot}4EtOH{\cdot}3H_2O$. Elemental analysis calcd. for $C_{37}H_{63}N_5O_{20}Cu_2$: C, 43.64%, H, 6.20%, N, 6.83%; found: C, 43.49%, H, 6.21%, N, 6.74%; selected FTIR (KBr, cm^{-1}): 1657, 1637, 1495, 1448, 1414, 1379, 1254, 1159, 1095, 775, 760, 729.

ZJNU-48: A mixture of H_4L3 (5.0 mg, 12.2 μmol), and $Cu(NO_3)_2{\cdot}3H_2O$ (15.0 mg, 62.1 μmol) was dissolved in a mixed solvent of DMF (1.5 mL), CH_3CN (0.5 mL), and H_2O (0.08 mL) in a 20 mL glass vial. After the addition of 6 M HCl (30 μL), the vial was sealed and heated to 353 K for 72 h and then cooled to room temperature. The block-shaped crystals formed were collected by filtration in 56% yield. Based on the single-crystal X-ray structural determination, TGA and elemental analysis, **ZJNU-48** can be best formulated as $[Cu_2L3(H_2O)_2]{\cdot}3DMF{\cdot}4CH_3CN{\cdot}3H_2O$. Elemental analysis calcd. for $C_{37}H_{51}N_9O_{16}Cu_2$: C, 44.22%, H, 5.12%, N, 12.54%; Found: C, 44.11%, H, 5.06%, N, 12.57%; selected FTIR (KBr, cm^{-1}): 1660, 1635, 1593, 1452, 1394, 1365, 1323, 1254, 1095, 775, 760, 729.

2.4 Crystal structure determination

Intensity data for **ZJNU-46** and **ZJNU-48** were collected at 296(2) K on a Bruke SMART APEX II CCD area-detector diffractometer using graphite monochromated Mo-K_a radiation (λ = 0.71073 Å). The structures were solved by direct methods using the program SHELXS-97. All non-hydrogen atoms were refined anisotropically by full matrix least-squares methods using SHELXL-97. The unit cell includes a large region of disordered solvent molecules which could not be modelled as discrete atomic sites. We employed PLATON/SQUEEZE[15] to calculate the diffraction contribution of solvent molecules and thereby to produce a set of solvent-free diffraction intensities. The resulting new files were used to further refine the structures. The H atoms on C atoms were generated geometrically. Crystal data and structure refinement parameters for the two compounds are presented in Table S1 in the supporting information.

2.5 Calculation of Isosteric heat of C_2H_2 adsorption

The isosteric heat of C_2H_2 adsorption, Q_{st}, was calculated using the Clausius-Clapeyron equation, expressed as

$$Q_{st} = -R\left(\frac{\partial \ln P}{\partial (1/T)}\right)_q \quad (4)$$

where *P* is the pressure, *T* is the temperature, *R* is the gas constant, and *q* is the adsorption amount. Linear fitting of ln*P* versus 1/*T* for the C_2H_2 adsorption was provided in Fig. S5 in the supporting information. The slope of Inp~1/T was derived from the fitted line, and Q_{st} was calculated from the above equation.

3. Results and Discussions

3.1 Synthesis and characterization

The organic linkers H_4L1 and H_4L3 were readily synthesized by Palladium-catalyzed Suzuki cross-coupling between dimethyl 5-(pinacolboryl)isophthalate and the corresponding dihalo compounds, 2,5-dibromopyrazine and 5-bromo-2-iodopyrimidine, followed by hydrolysis and acidification. The detailed synthesis procedures are shown in experimental section. The chemical structures of the organic linkers and their intermediates were characterized by NMR spectroscopy. Solvothermal reaction between the organic ligand H_4L1 and $Cu(NO_3)_2{\cdot}3H_2O$ in a DMF/EtOH/H_2O mixed solvent under acidic conditions at 353 K for 24 h afforded blue block-shaped crystals of **ZJNU-46**, while **ZJNU-48** was obtained as blue block-shaped crystals by a solvothermal reaction of H_4L3 and $Cu(NO_3)_2{\cdot}3H_2O$ in a DMF/CH_3CN/H_2O mixed solvent with the addition of a small amount of HCl at 353 K for 72 h. Their structures were characterized by single-crystal X-ray diffraction and the phase purity of the bulk materials was independently confirmed by powder X-ray diffraction experiments showing that the measured PXRD patterns closely match the simulated ones generated from single-crystal diffraction data (Fig. S1 in the supporting information). Based on the single-crystal X-ray diffraction studies, TGA (Fig. S2) and elemental analysis, **ZJNU-46** and **ZJNU-48** can be best formulated as $[Cu_2L1(H_2O)_2]{\cdot}3DMF{\cdot}4EtOH{\cdot}3H_2O$ and $[Cu_2L3(H_2O)_2]{\cdot}3DMF{\cdot}4CH_3CN{\cdot}3H_2O$, respectively.

3.2 Structural description

Single-crystal X-ray diffraction analysis showed that **ZJNU-46**

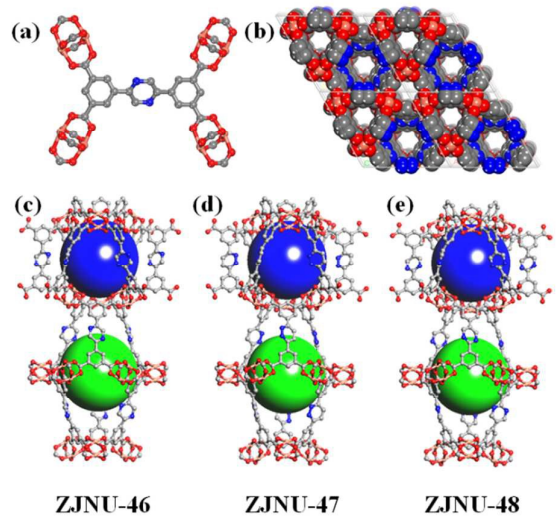

Fig. 1 Single-crystal X-ray structure of **ZJNU-46** showing the coordination environment of the organic linker $L1^{4-}$ (a), and 3D packing diagram along the *c* axis (b). Two different types of nanocages observed in **ZJNU-46** (c), **ZJNU-47** (d) and **ZJNU-48** (e). Hydrogen atoms and the terminal water molecules are omitted for clarity.

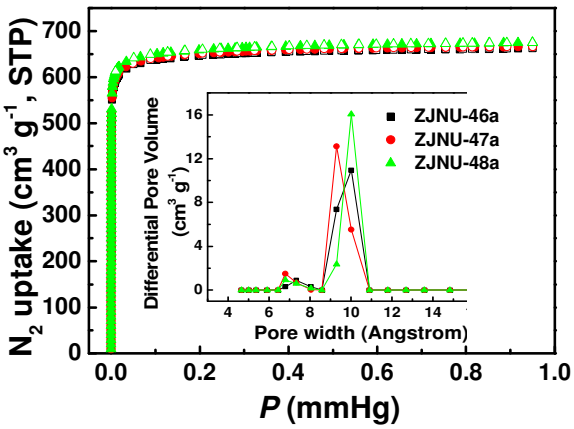

Fig. 2 N_2 adsorption-desorption isotherms of **ZJNU-46a**, **ZJNU-47a** and **ZJNU-48a** at 77 K. Solid and open symbols represent adsorption and desorption, respectively. The inset exhibits pore size distribution of the three compounds.

and **ZJNU-48** are isostructural with **ZJNU-47**, crystallizing in the space group of *R*-3m. The crystal structure of **ZJNU-46** was representatively described. The two adjacent copper ions were bridged by four carboxylate groups from four different organic ligands to form dicopper paddlewheel $[Cu_2(COO)_4]$ SBUs which are further connected by the organic linkers to form a three-dimensional (3D) NbO-type structure with the Schläfli topological symbol of $\{6^4{\cdot}8^2\}$ in which the dicopper SBU and the organic linker are taken as 4-connected node, respectively (Fig. 1a,b). Two different types of nanocages can be observed which are alternatively stacked with each other along the *c* axis by sharing three dicopper paddlewheel SBUs. The small cage of about 11 Å in diameter, indicated by the blue sphere, is encapsulated by six paddlewheel clusters and twelve organic ligands, while the large irregular and elongated cage of *ca.* 12×21 Å, shown in green sphere, is surrounded by twelve dicopper clusters and six organic ligands. The cage surface was decorated with potential open copper sites and Lewis basic nitrogen donor sites, which is favourable for gas adsorption. PLATON calculations indicate that the total accessible volumes of the three MOFs after removal of the guest and coordinated water molecules are 68.6%, 67.5%, and 69.5% for **ZJNU-46**, **ZJNU-47** and **ZJNU-48**, respectively. By comparison, the difference between the three compounds is only the relative position of nitrogen atoms on the spacers of the organic ligands (Fig. 1c-e).

3.3 Permanent porosity

In order to characterize pore structure, we measured N_2 adsorption-desorption isotherms at 77 K. Prior to measurements, the as-synthesized samples were solvent exchanged with dry acetone and evacuated under dynamic vacuum at 373 K until the degassed rate reached 2 μmHg min^{-1}, affording the activated samples. As shown in Fig. 2, the three compounds exhibit type-I reversible sorption isotherms *as per* the IUPAC classification, characteristic of microporous materials. The maximum N_2 uptakes at 77 K are 663, 666 and 675 cm^3 (STP) g^{-1} for **ZJNU-46a**, **ZJNU-47a** and **ZJNU-48a**, respectively. Based on the N_2 adsorption isotherms, the BET (Langmuir) surface areas were calculated to be 2622 (2883), 2638 (2902) and 2670 (2922) m^2 g^{-1} for **ZJNU-46a**, **ZJNU-47a** and **ZJNU-48a**, respectively (Fig. S3), which are comparable to that of NOTT-101.[16] The pore volumes calculated from the maximum N_2 uptakes are 1.025, 1.031 and 1.044 cm^3 g^{-1} for **ZJNU-46a**, **ZJNU-47a** and **ZJNU-48a**, respectively, which are close to the theoretical values of 0.996, 0.979 and 0.998 cm^3 g^{-1} calculated using PLATON software. The inset in Fig. 2 exhibits that the three compounds have the similar pore size distribution. By comparison, it is clear that the three compounds have almost the same porosities, regardless of the relative position of the nitrogen atoms in the spacers between the terminal isophthalate moieties of the organic linkers.

3.4 C_2H_2 sorption isotherms

Considering that the three compounds feature the uncoordinated Lewis basic nitrogen sites and Lewis acidic copper sites after activation, we explored their acetylene adsorption properties. Accordingly, acetylene gas isotherms were measured at five different temperatures of 278 K, 288 K, 295 K, 298 K and 308 K, which were shown in the Fig. 3. No apparent hysteresis between adsorption and desorption is observed, indicating the fast adsorption and desorption kinetics. At 295 K and 1 atm, the gravimetric acetylene uptakes are 187, 213 and 193 cm^3 (STP) g^{-1} for **ZJNU-46a**, **ZJNU-47a** and **ZJNU-48a**, respectively. When the temperature goes down from 295 K to 278 K, the amount of acetylene adsorbed increased to 257, 283 and 265 cm^3 (STP) g^{-1}, respectively. The acetylene adsorption amounts for the three compounds are significantly higher than those for carbon molecular sieves[17], mesoporous silica,[18] cucurbit[6]uril,[19] *p*-tert-butylcalix[4]arene,[20] and hydrogen-bonded organic framework material HOF-1[21] under the same conditions. For comparison, acetylene adsorption data for several typical microporous

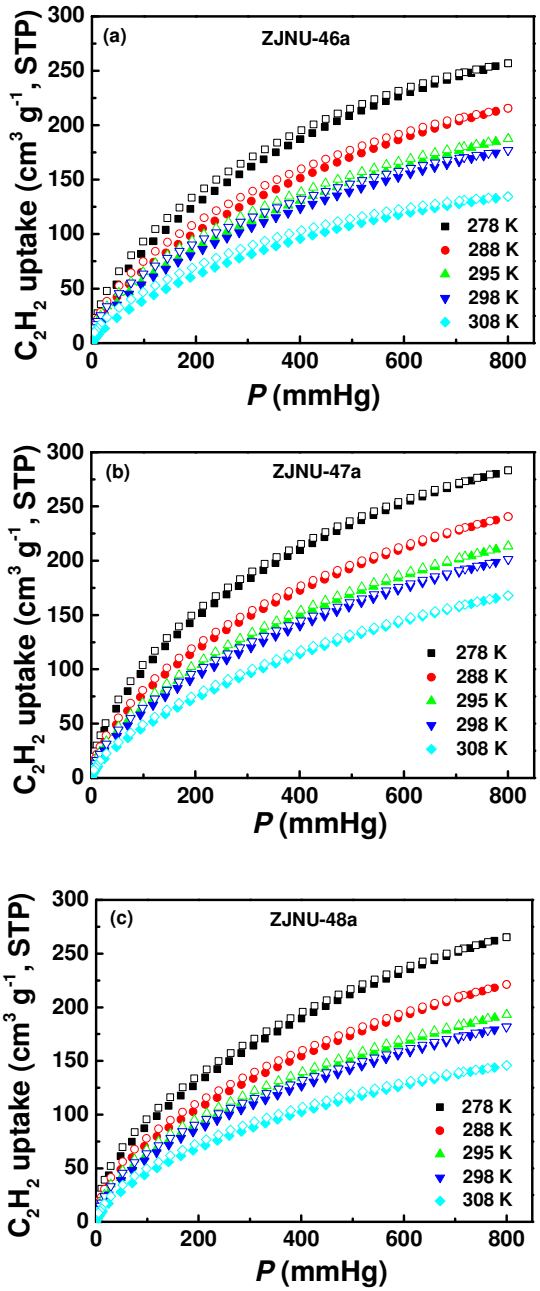

Fig. 3 C_2H_2 adsorption isotherms of **ZJNU-46a** (a), **ZJNU-47a** (b) and **ZJNU-48a** (c) at five different temperatures. Solid and open symbols represent adsorption and desorption, respectively.

MOFs are compiled in Table 1. It can be observed that the gravimetric C_2H_2 adsorption amount of **ZJNU-47a** is the second highest reported for MOF materials, and is only lower than that of FJI-H8.[11] The storage density of acetylene in the bulk material **ZJNU-47a** at 295 K reaches 0.17 g cm^{-3}, which is equivalent to the density of acetylene at 16.2 MPa at 298 K and is 81 times larger than the value of the compression limit for the safe storage of acetylene at room temperature. Furthermore, the C_2H_2 storage capacities of **ZJNU-47a** are still

Table 1 Comparison of acetylene adsorption data at ambient temperature and 1 bar for some typical MOFs

MOFs	C_2H_2 uptake (cm^3 g^{-1})	Q_{st} (kJ mol^{-1})	BET (m^2 g^{-1})	V_p (cm^3 g^{-1})	*Ref.*
FJI-H8	224[c]	32.0	2025	0.82	[11]
ZJNU-47	213[c]	35.0	2638	1.031	This work
HKUST-1	201[c]	30.4	1401	0.760	[9]
CoMOF-74	197[c]	50.1	1018	NA	[10]
ZJU-5	193[a]	35.8	2823	1.074	[12]
ZJNU-48	193[c]	33.0	2670	1.044	This work
ZJNU-46	187[c]	26.9	2622	1.025	This work
Cu-EBTC	160[c]	34.5	1852	1.000	[8k]

[a] 298 K; [b] 296 K; [c] 295 K

not saturated in the pressure range investigated, which means that the C_2H_2 uptake can be further maximized until the limit of safe storage of acetylene under a pressure of 2 atm. By fitting the acetylene adsorption data with Langmuir-Freundlium equation (R^2 = 0.99995, Fig. S4), acetylene uptake at 295 K and 2 atm was predicted to be 284 cm^3 (STP) g^{-1}.

The most striking feature is that the amounts of acetylene adsorbed by the three compounds differ significantly, and the compound **ZJNU-47a** exhibited much higher acetylene uptakes than the other two compounds **ZJNU-46a** and **ZJNU-48a** although they feature the same porosities, pore size distributions, and densities of OMSs and uncoordinated nitrogen sites. To figure out the underlying reason, the coverage-dependent enthalpies of acetylene adsorption were calculated based on the Clausius-Claperyron equation from the adsorption isotherms collected at 278 K, 288 K and 298 K. As shown in Fig. 4, the adsorption enthalpies of acetylene at low coverage (4.0 cm^3 g^{-1}) are 26.9, 35.0 and 33.0 kJ mol^{-1} for **ZJNU-46a**, **ZJNU-47a** and **ZJNU-48a**, respectively, which are significantly higher than the latent enthalpy of vaporization for acetylene of 20.9 kJ mol^{-1}. The adsorption enthalpies of acetylene at low coverage for **ZJNU-47a** are comparable to those for FJI-H8[11] and HKUST-1[9], but lower than that for MOFs with high density of open metal sites such as CoMOF-74.[10] With the increase in coverage, the heats of acetylene adsorption of the three compounds show downward trend, and then begin to slowly increase. The latter trend might be attributed to attractive C_2H_2-C_2H_2 interaction, which becomes important at higher loadings. More importantly, **ZJNU-47a** exhibits even higher adsorption enthalpies of C_2H_2 than the other two compounds. The reason for such higher adsorption enthalpies within **ZJNU-47a** is still not very clear at this moment, as apparently these three MOFs have quite similar OMSs, uncoordinated nitrogen sites and pore size distribution. We speculated that the arrangement of these nitrogen sites and their orientation with respect to each other play crucial roles in such differential interactions with acetylene guest molecules. In fact, Wang *et al.* also demonstrated that the unique alignment of open copper sites in MOFs is capable of enhancing H_2 uptake.[22] In our cases, compared to the separated nitrogen atoms in **ZJNU-46a** and **ZJNU-48a,** the adjacent ones presented in **ZJNU-47a** might play a synergistic

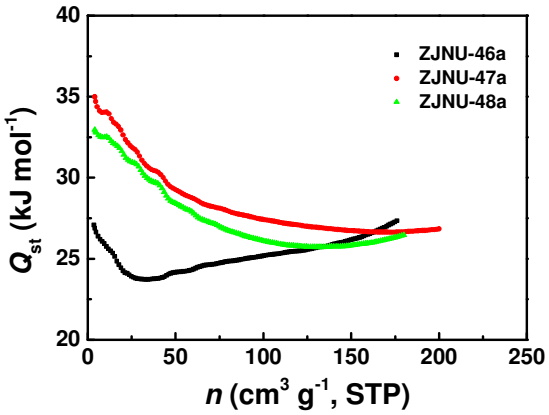

Fig. 4 Coverage-dependence of isosteric heats of acetylene adsorption on the three MOFs **ZJNU-46a**, **ZJNU-47a** and **ZJNU-48a**.

role, which enforces their stronger interactions with the adsorbed acetylene molecules. The high affinity of **ZJNU-47a** toward acetylene is thus responsible for the greater acetylene uptake capacity of **ZJNU-47a** under ambient conditions. This also demonstrates that the rational design of open nitrogen sites will favourably boost the acetylene gas sorption capacities.

4 Conclusion

The acetylene sorption properties of three isostructural NbO-type MOFs were systematically studied, exhibiting exceptionally high sorption capacities with regard to acetylene due to the simultaneous immobilization of open metal sites, Lewis basic nitrogen sites in the frameworks. The gravimetric acetylene uptake of the compound **ZJNU-47** is the second highest one reported so far. Although they have the same porosities, and densities of open metal sites and Lewis basic nitrogen sites, the difference in the relative position of the nitrogen atoms in the spacer between the terminal isophthalate moieties in the organic linkers leads to their distinctly different acetylene uptake capacities. This work demonstrates that the rational design of nitrogen sites will favourably increase acetylene uptake and thus provides useful information for the future design of MOFs for acetylene storage.

Acknowledgement

This work was supported by the National Natural Science Foundation of China (No. 21301156), and Qianjiang talents project in Zhejiang province (ZC304015017).

Notes and references

1 (a) B. Chen, S. Ma, E. J. Hurtado, E. B. Lobkovsky and H.-C. Zhou, *Inorg. Chem.*, 2007, **46**, 8490-8492; (b) A. H. Assen, Y. Belmabkhout, K. Adil, P. M. Bhatt, D.-X. Xue, H. Jiang and M. Eddaoudi, *Angew. Chem. Int. Ed.*, 2015, **54**, 14353-14358.

2 (a) C. Song, Y. Ling, L. Jin, M. Zhang, D.-L. Chen and Y. He, *Dalton Trans.*, 2016, **45**, 190-197; (b) C. Song, Y. He, B. Li, Y. Ling, H. Wang, Y. Feng, R. Krishna and B. Chen, *Chem. Commun.*, 2014, **50**, 12105-12108.

3 (a) M. P. Suh, H. J. Park, T. K. Prasad and D.-W. Lim, *Chem. Rev.*, 2012, **112**, 782-835; (b) L. J. Murray, M. Dincă and J. R. Long, *Chem. Soc. Rev.*, 2009, **38**, 1294-1314.

4 (a) C. Song, Y. Ling, Y. Feng, W. Zhou, T. Yildirim and Y. He, *Chem. Commun.*, 2015, **51**, 8508-8511; (b) Y. He, W. Zhou, G. Qian and B. Chen, *Chem. Soc. Rev.*, 2014, **43**, 5657-5678; (c) Y. He, W. Zhou, T. Yildirim and B. Chen, *Energy Environ. Sci.*, 2013, **6**, 2735-2744; (d) T. A. Makal, J.-R. Li, W. Lu and H.-C. Zhou, *Chem. Soc. Rev.*, 2012, **41**, 7761-7779; (e) K. Konstas, T. Osl, Y. Yang, M. Batten, N. Burke, A. J. Hill and M. R. Hilla, *J. Mater. Chem.*, 2012, **22**, 16698-16708.

5 (a) Z. Zhang, Y. Zhao, Q. Gong, Z. Li and J. Li, *Chem. Commun.*, 2013, **49**, 653-661; (b) K. Sumida, D. L. Rogow, J. A. Mason, T. M. McDonald, E. D. Bloch, Z. R. Herm, T.-H. Bae and J. R. Long, *Chem. Rev.*, 2012, **112**, 724-781.

6 (a) Z. R. Herm, E. D. Bloch and J. R. Long, *Chem. Mater.*, 2014, **26**, 323-338; (b) Y. He, W. Zhou, R. Krishna and B. Chen, *Chem. Commun.*, 2012, **48**, 11813-11831; (c) H. Wu, Q. Gong, D. H. Olson and J. Li, *Chem. Rev.*, 2012, **112**, 836-868; (d) Z. Zhang, S. Xiang and B. Chen, *CrystEngComm*, 2011, **13**, 5983-5992.

7 R. Matsuda, R. Kitaura, S. Kitagawa, Y. Kubota, R. V. Belosludov, T. C. Kobayashi, H. Sakamoto, T. Chiba, M. Takata, Y. Kawazoe and Y. Mita, *Nature*, 2005, **436**, 238-241.

8 (a) Q.-G. Zhai, N. Bai, S. n. Li, X. Bu and P. Feng, *Inorg. Chem.*, 2015, **54**, 9862-9868; (b) J. Duan, W. Jin and R. Krishna, *Inorg. Chem.*, 2015, **54**, 4279-4284; (c) T. Xia, J. Cai, H. Wang, X. Duan, Y. Cui, Y. Yang and G. Qian, *Micropor. Mesopor. Mater.*, 2015, **215**, 109-115; (d) J. Li, H.-R. Fu, J. Zhang, L.-S. Zheng and J. Tao, *Inorg. Chem.*, 2015, **54**, 3093-3095; (e) K. Liu, B. Li, Y. Li, X. Li, F. Yang, G. Zeng, Y. Peng, Z. Zhang, G. Li, Z. Shi, S. Feng and D. Song, *Chem. Commun.*, 2014, **50**, 5031-5033; (f) S.-J. Lee, J. W. Yoon, Y.-K. Seo, M.-B. Kim, S.-K. Lee, U.-H. Lee, Y. K. Hwang, Y.-S. Bae and J.-S. Chang, *Microporous Mesoporous Mater.*, 2014, **193**, 160-165; (g) R. B. Getman, Y.-S. Bae, C. E. Wilmer and R. Q. Snurr, *Chem. Rev.*, 2012, **112**, 703-723; (h) E. D. Bloch, W. L. Queen, R. Krishna, J. M. Zadrozny, C. M. Brown and J. R. Long, *Science*, 2012, **335**, 1606-1610; (i) N. Nijem, H. Wu, P. Canepa, A. Marti, J. Kenneth J. Balkus, T. Thonhauser, J. Li and Y. J. Chabal, *J. Am. Chem. Soc.*, 2012, **134**, 15201-15204; (j) J.-P. Zhang and X.-M. Chen, *J. Am. Chem. Soc.*, 2009, **131**, 5516-5521; (k) Y. Hu, S. Xiang, W. Zhang, Z. Zhang, L. Wang, J. Bai and B. Chen, *Chem. Commun.*, 2009, 7551-7553; (l) D. G. Samsonenko, H. Kim, Y. Sun, G.-H. Kim, H.-S. Lee and K. Kim, *Chem. Asian J.*, 2007, **2**, 484-488.

9 S. Xiang, W. Zhou, J. M. Gallegos, Y. Liu and B. Chen, *J. Am. Chem. Soc.*, 2009, **131**, 12415-12419.

10 S. Xiang, W. Zhou, Z. Zhang, M. A. Green, Y. Liu and B. Chen, *Angew. Chem. Int. Ed.*, 2010, **49**, 4615-4618.

11 J. Pang, F. Jiang, M. Wu, C. Liu, K. Su, W. Lu, D. Yuan and M. Hong, *Nat. Commun.*, 2015, **6**, 7575.

12 X. Rao, J. Cai, J. Yu, Y. He, C. Wu, W. Zhou, T. Yildirim, B. Chen and G. Qian, *Chem. Commun.*, 2013, **49**, 6719-6721.

13 C. Song, J. Hu, Y. Ling, Y. Feng, D.-L. Chen and Y. He, *Dalton Trans.*, 2015, **44**, 14823 -14829.

14 B. Li, H.-M. Wen, H. Wang, H. Wu, M. Tyagi, T. Yildirim, W. Zhou and B. Chen, *J. Am. Chem. Soc.*, 2014, **136**, 6207-6210.

15 A. L. Spek, *J. Appl. Crystallogr.*, 2003, **36**, 7–13.

16 (a) X. Lin, I. Telepeni, A. J. Blake, A. Dailly, C. M. Brown, J. M. Simmons, M. Zoppi, G. S. Walker, K. M. Thomas, T. J. Mays, P. Hubberstey, N. R. Champness and M. Schröder, *J. Am. Chem. Soc.*, 2009, **131**, 2159-2171; (b) X. Lin, J. Jia, X. Zhao, K. M. Thomas, A. J. Blake, G. S. Walker, N. R. Champness, P. Hubberstey and M. Schröder, *Angew. Chem. Int. Ed.*, 2006, **45**, 7358-7364.
17 C. R. Reid and K. M. Thomas, *Langmuir*, 1999, **15**, 3206-3218.
18 B. L. Newalkar, N. V. Choudary, U. T. Turaga, R. P. Vijayalakshmi, P. Kumar, S. Komarneni and T. S. G. Bhat, *Microporous Mesoporous Mater.*, 2003, **65**, 267-276.
19 S. Lim, H. Kim, N. Selvapalam, K.-J. Kim, S. J. Cho, G. Seo and K. Kim, *Angew. Chem. Int. Ed.*, 2008, **47**, 3352-3355.
20 P. K. Thallapally, L. Dobrzańska, T. R. Gingrich, T. B. Wirsig, L. J. Barbour and J. L. Atwood, *Angew. Chem. Int. Ed.*, 2006, **45**, 6506-6509.
21 Y. He, S. Xiang and B. Chen, *J. Am. Chem. Soc.*, 2011, **133**, 14570-14573.
22 X.-S. Wang, S. Ma, P. M. Forster, D. Yuan, J. Eckert, J. J. L-pez, B. J. Murphy, J. B. Parise and H.-C. Zhou, *Angew. Chem. Int. Ed.*, 2008, **47**, 7263-7266.

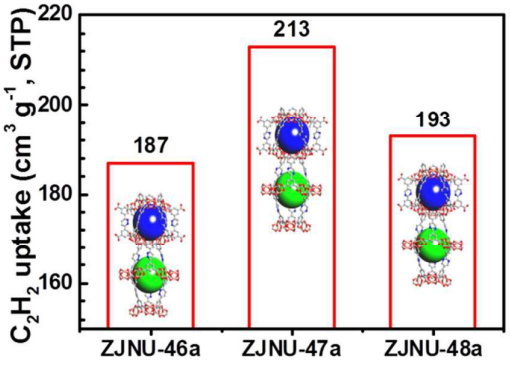

Rational arrangement of nitrogen sites in metal-organic frameworks with the same structure is capable of boosting acetylene adsorption.